European Review for Medical and Pharmacological Sciences 2014; 18: 3601-3610

Binary logistic regression analysis of solid thyroid nodules imaged by high-frequency ultrasonography, acoustic radiation force impulse, and contrast-enhanced ultrasonography

X.-N. LIANG[1], R.-J. GUO[1], S. LI[1], Z.-M. ZHENG[2], H.-D. LIANG[3,4]

[1]Department of Ultrasound Medicine, Beijing Chaoyang Hospital, Capital Medical University, China.
[2]The First Hospital of Shijiazhuang City, China.
[3]Institute of Medical Engineering and Medical Physics, School of Engineering, Cardiff University, Cardiff, UK.
[4]Information Science and Engineering School, Fudan University, Shanghai, China

Abstract. – OBJECTIVE: The common clinical techniques used for examining thyroid tumors include palpation, imaging, immunoassays and tissue biopsy. Ultrasonography is easy, non-invasive, non-radioactive and highly reproducible imaging technique; however, due to the disease polytropism, diagnosis may become difficult sometimes. Ultrasound elastography, particularly acoustic radiation force impulse (ARFI) imaging and contrast-enhanced ultrasonography (CEUS) have been successfully used to diagnose the thyroid tumors. The objective of this retrospective study was to analyze and compare the solid thyroid nodules imaged by high-frequency ultrasonography (HFUS), ARFI imaging, and CEUS.

PATIENTS AND METHODS: For this purpose, images of the 80 solid thyroid nodules (58 benign and 22 malignant) with surgical pathology were obtained and data were compared using binary logistic regression analysis.

RESULTS: Morphology ($p < 0.001$), and internal calcification ($p = 0.007$) were statistically different. The mean shear wave velocity (SWV) measured by ARFI was significantly different ($p = 0.029$). Three sets of comparison on CEUS ($p = 0.019$) and time to peak (TTP) of CEUS were significantly different ($p = 0.001$). The logistic regression analysis indicated that the morphology, mean SWV of ARFI and TTP were independent risk factors for malignancy. The diagnostic accuracy for solid thyroid nodules was 85.1% (68/80) and the area under the receiver operating characteristic (ROC) curve was 0.945±0.033.

CONCLUSIONS: Logistic regression analysis can effectively screen significant parameters for the differential diagnosis of solid thyroid nodules imaged by ultrasonography.

Key words:
Binary logistic regression, Thyroid nodule, High-frequency ultrasonography, Acoustic radiation force impulse, Contrast-enhanced ultrasonography.

Introduction

At present, the most common clinical techniques for examining the thyroid include palpation, imaging, immunological assays and tissue biopsy. High-frequency ultrasonography (HFUS) can detect thyroid nodules >3 mm in diameter and provide clear images of the thyroid and surrounding tissue. Ultrasonography also facilitates the dynamic real-time observation of lesions. Moreover, it is non-invasive, easy to perform, non-radioactive and highly reproducible. These advantages have made ultrasonography the preferred thyroid imaging technique[1]. Gray-scale ultrasonography (GSUS), color Doppler ultrasonography (CDUS) and B-mode dimensional ultrasonography (DUS) are valuable for identifying benign and malignant thyroid nodules. However, due to the polytropism of this disease, diagnosis remains difficult in some cases. In recent years, ultrasound elastography, particularly acoustic radiation force impulse (ARFI) imaging and contrast-enhanced ultrasonography (CEUS) have also been used to diagnose the benign and malignant thyroid nodules[2].

Herein, we compared the appearance and perfusion patterns of solid thyroid nodules detected by HFUS, ARFI, and CEUS, together with the

Corresponding Author: Rui-Jun Guo, MD; e-mail: guodaoshi@126.com

findings from pathological analyses, and performed a binary logistic regression analysis to identify the risk factors for malignancy.

Patients and Methods

Patients

This study analyzed the data from 80 patients in whom thyroid gland tubercles were identified at routine ultrasonic scan at our hospital during the time period from January to May 2013. The subjects included 45 males and 35 females, aged 19-62 (30±5.5) years. These 80 patients were suspected for thyroid cancer after conventional ultrasonography examination. Subsequently, 90 large, solid nodules from these patients were subjected to ARFI, CEUS, as well as pathological examination, and 80 of these tumors were included in this analysis. Inclusion criteria were as follows: (1) nodules that manifested as solid nodules or with a >75% solid component on ultrasonography; (2) nodules that were subjected to ARFI and CEUS examination; and (3) nodules that were also assessed by histopathological examination. A total of 41 nodules were located in the left lobe, 30 were in the right lobe and 9 were in the isthmus. The nodular diameter was 19.1±21.1 mm (range: 5.0-56.0 mm).

We received written informed consent from each person for data inclusion in our analysis and the study was approved by Capital Medical University's Ethics Committee.

HFUS, ARFI and CEUS Examinations

HFUS and ARFI examinations were performed using Siemens Acuson S2000 Color Doppler ultrasonography, ARFI imaging software, and a linear probe with frequency of 6.0-10.0 MHz and a center frequency of 7.5 MHz (Siemens Acuson S2000, Siemens, Berlin, Germany).

For HFUS examination, patients lay in the supine position with their neck fully exposed. They were instructed to remain calm and breathe evenly as images of the nidus were obtained by GSUS and CDUS. To facilitate comparison of the preoperative ultrasonography and postoperative pathological findings, the location of each nodule was recorded as follows: left or right lobe, isthmus; upper, middle and lower pole; ventral or dorsal. Echogenicity, morphology, border, acoustic halo, and calcification characteristics of the nodules were also recorded. The echogenicity of the nodules was classified as hyper-, iso-, hypo- and extremely hypo- with regard to adjacent thyroid parenchyma and the anterior muscle. Hyper-echogenicity was higher than that of adjacent thyroid parenchyma; iso-echogenicity was close to that of the normal thyroid parenchyma; hypo-echogenicity was above that of the anterior muscle but below the normal thyroid parenchyma and extremely hypo-echogenicity was close to or below that of the anterior muscle. TGC curve was set higher in deep tissue and lower in superficial tissue, usually in a linear manner. The same operator had performed the scans to ensure the consistency in TGC setting. Morphologically, nodules were classified as oval (the anteroposterior diameter of the nodule was smaller than the transverse diameter) with an aspect ratio >1 or <1 or irregular (all sizes barring those described above). The nodular border was classified as clear (nodular surface was smooth and clearly distinguishable from the surrounding tissues) or unclear (the boundaries between the nodule and surrounding tissues were obscure). The acoustic halo around the nodule was classified as regular (curved or ring-like with a constant thickness and a smooth outline) or irregular (uneven thickness and incomplete outline). Calcification was categorized as microcalcification (calcified spot diameter <1 mm) or coarse calcification (calcified spot diameter >1 mm).

Regarding ARFI examination, there are two forms of ARFI imaging i.e. Virtual Touch Imaging (VTI) and Virtual Touch Quantification (VTQ). The VTI image shows only the relative hardness in grayscale with no absolute value. The comparison was based on the human eye judgment and it did not involve computer-aided quantification. This was similar to conventional ultrasonic elasticity imaging (EI), but the difference was that no external pressure was applied and the probe gently touched the skin surface with the system switched to VTI mode. The region of interest (ROI) was adjusted to be more than twice the size of the lesions in the B-mode imaging. ROI was placed at the center of nodules to avoid the cyst or calcification. The EI was classified using Ueno and Ito elasticity scores[3] as follows: Score 1: white in the whole nodule. Score 2: white in a large part of the nodule. Score 3: white and black in half of the nodule. Score 4: black in a large part of the nodule. Score 5: black in the

whole nodule. Scores 4 and 5 were regarded as the malignant thyroid nodule, and scores 1-3 were regarded as benign thyroid nodule. The VTQ calculated the value of the ROI transverse shear wave velocity (SWV) automatically. The location, direction, and depth of the probe were maintained at the same nodule and 5 measurements were taken. The highest and lowest values were discarded and the remaining 3 values were averaged. The SWV was considered proportional to the square root of tissue elasticity and was expressed as m/s. If the VTI mainly appeared as black, then all the VTQ values were set to 9 m/s. If the nodule was too hard or too soft, a value was not obtained as the detectable range of SWV is 0-9.99 m/s[4,5].

For CEUS examination, a Philip iU22 color Doppler scanner (Philip iU22, Philip, Amsterdam, Holland) with a probe frequency of 9-12MHz and a mechanical index (MI) of 0.08 was used. SonoVue (Sulphur hexafluoride, Bracco, Milan, Italy) contrast agent was dissolved in 5mL of saline solution and shaken to form microbubbles in suspension as described[6]. Conventional ultrasonography was first employed for scanning of the thyroid, surrounding tissues, and lymph nodes; and later, selected nodules were measured (before CEUS mode was initiated). The operator tried to keep observation section constant, rapidly injected 2.4 mL of the mixture of contrast agents, and then flushed with 5 mL saline. Meantime, the operator initiated timer, continuously observed the dynamic perfusion process with observation time ≥120s and saved images. The images were classified into the following three enhancement patterns: homogeneous, heterogeneous, or ring-enhancing[7]. Time-intensity curves within the selected ROI and color maps were acquired. Nodule and normal thyroid parenchyma values of peak contrast enhancement (Peak) and time to peak (TTP) were calculated. Peak and TTP were reported as indexes (Peak index, TTP index) derived from the ratio between the values from the ROI of nodule and the ROI of normal thyroid parenchyma[8]. We calculated the ratio as >1 or <1.

Statistical Analysis

Pathology was regarded as the gold standard diagnostic technique. SPSS13.0 statistical software (Statistical Product and Service Solutions, IBM, New York, USA) was used for all statistical analyses of the quantitative data expressed as average±standard deviation (x±SD) values. VTI and SWV, Peak and TTP of CEUS, border characteristics, acoustic halo, morphology, echogenicity, and calcification were treated as independent variables (inclusion criteria: $p < 0.05$, exclusion criteria: $p > 0.10$). Binary logistic regression analysis was used to determine associations between surgical pathological findings of benignancy and malignancy and these variables. The forward stepwise method of regression was used along with likelihood ratios (Table I). The regression p-value was used to identify the benign and malignant nodules as follows: $p > 0.5$ was defined as malignant and $p \leq 0.5$ was defined as benign. Adopting Wald's χ^2-test for the regression parameter estimation, a odds ratio (OR value) was applied to test and evaluate the fit of each condition in the model (OR value of >1 was defined as a risk factor). Sensitivity and specificity were evaluated with the available histological data. After HFUS, we arbitrarily considered nodules with scores 3-5 and malignant histology to be true positives (TP) and nodules with scores 1-2 and benign histology to be true negatives (TN). Nodules with scores 3-5 and benign histology were regarded as false positives (FP) while nodules with scores 1-2 and malignant histology were regarded as false negatives (FN). After VTI with ARFI, nodules with scores 4-5 and malignant histology were considered to be TP while those with scores 1-3 and benign histology were considered to be TN. Nodules with scores 4-5 and benign histology were classified as FP and those with scores 1-3 and malignant histology were regarded as FN. Nodules with SWV >3.65±0.22 ms^{-1} and malignant histology were treated as TP. Nodules with SWV <2.01±1.25 $ms^{-1}$and benign histology were considered as TN. Nodules with SWV >3.65±0.22 $ms^{-1}$and benign histology were regarded as FP. Nodules with SWV <2.01±1.25 ms^{-1} and malignant histology were considered FN. After CEUS, nodules with a Peak index of ≤1 and/or TTP index of ≥1 and malignant histology were deemed as TP while those with a Peak index of >1 and/or TTP index of <1 and benign histology were deemed as TN. Nodules with a Peak index of ≤1 and/or TTP index of ≥1 and benign histology were classified as FP and those with a Peak index of >1 and/or TTP index of <1 and malignant histology were considered FN. Sensitivity and specificity were determined as follows[8]:

- Sensitivity = TP/ (TP+FN)
- Specificity = TN/ (TN+FP)

Results

Surgical and Pathological Findings

All 80 nodules included in this study were subjected to postoperative pathological assessment according to which, 58 were classified as benign and 22 as malignant. The benign nodules included 39 nodular goiters and 19 adenomatous goiters. The malignant nodules included 18 papillary carcinomas and 4 medullary carcinomas. There were 7 cases of single cancer combined with a nodular goiter and 15 cases of multiple tumors combined with a nodular goiter.

HFUS Findings

The HFUS imaging analysis of benign and malignant thyroid nodules (Table II) revealed that the borders (clear or unclear) compared between benign and malignant nodules differed significantly ($p = 0.027$); acoustic halo (regular, irregular, no) differed non-significantly ($p = 0.061$); contrast among morphology (aspect ratio <1, aspect ratio >1, irregular) was statistically different ($p < 0.001$); contrast among echogenicity (hyper-, iso-, hypo-, extremely hypo-) was statistically different ($p = 0.007$); and contrast among calcification conditions (no, coarse, micro) inside nodules was also statistically different ($p < 0.001$). Figure 1A and B show the HFUS images of benign and malignant thyroid nodules, respectively.

VTI Classification and the SWV of VTQ Findings

There were 26 nodules with scores 4-5 and 54 nodules with scores 1-3 with regard to the VTI image contrast of nodules and their adjacent normal thyroid tissue. Figure 2A and B show the VTI images of benign and malignant thyroid nodules, respectively. The SWV values of benign and malignant nodules were 3.65±0.22 ms^{-1} and 2.01±1.25 ms^{-1}, respectively. The SWV values of

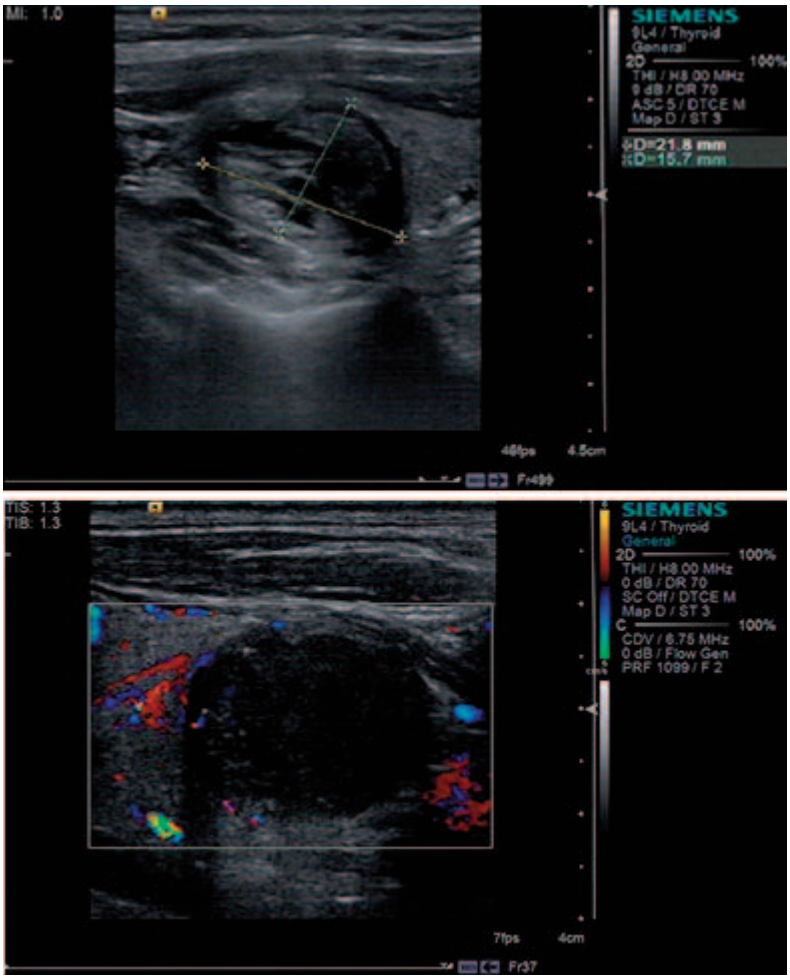

Figure 1. ***A,*** Gray-scale image of the malignant nodule; ***B,*** Color Doppler image of the benign nodule.

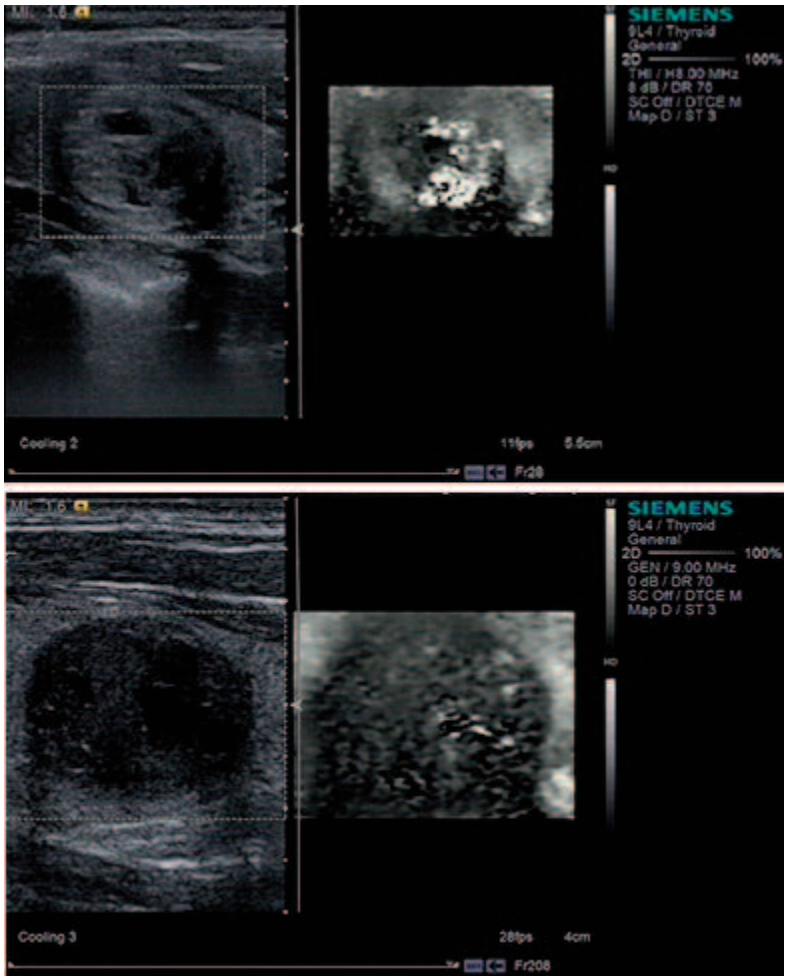

Figure 2. A, VTI image of the malignant nodule; **B,** VTI image of the benign nodule.

benign and malignant nodules were significantly different ($p = 0.029$). Figure 3A and B show the SWV values of VTQ of benign and malignant thyroid nodules, respectively.

CEUS findings

The CEUS features of thyroid nodule and normal thyroid tissue are summarized in Table III. The three sets of comparisons among homogeneous, heterogeneous and ring-enhancing nodule were statistically different ($p < 0.001$). Both heterogeneous vs. ring-enhancing nodules ($p < 0.001$) as well as homogeneous vs. heterogeneous nodules differed significantly ($p < 0.001$). The TTP between benign and malignant nodules also differed significantly ($p < 0.001$). Malignant nodules took less time than benign nodules to reach peak time; however, the peak value differed non-significantly. Figure 4A and B show the CEUS images of malignant nodules and the adjacent thyroid tissue, respectively. Time-intensity curve (TIC) analysis of the malignant nodule: ROI for red line was placed in the malignant nodule and yellow line was placed in the adjacent thyroid tissue.

Sensitivity and Specificity

The sensitivity and specificity values of HFUS were 95.4% and 74.1%, respectively. Comparing between two forms of ARFI, VTI had a higher sensitivity (VTI image sensitivity was 81.8%) than VTQ (SWV value for VTQ sensitivity was 77.3%) as well as a higher specificity (VTI image specificity was 82.8%) than VTQ (SWV of VTQ specificity was 55.5%) whereas the positive predictive value and accuracy were not as high. When VTI and VTQ were combined, the shunt sensitivity and specificity values were 91.7% and 50.0%, respectively. The values derived from VTI and VTQ of the benign and malignant thyroid nodules overlapped to some extent and, therefore, could not be regarded as a unique reference index when distinguishing be-

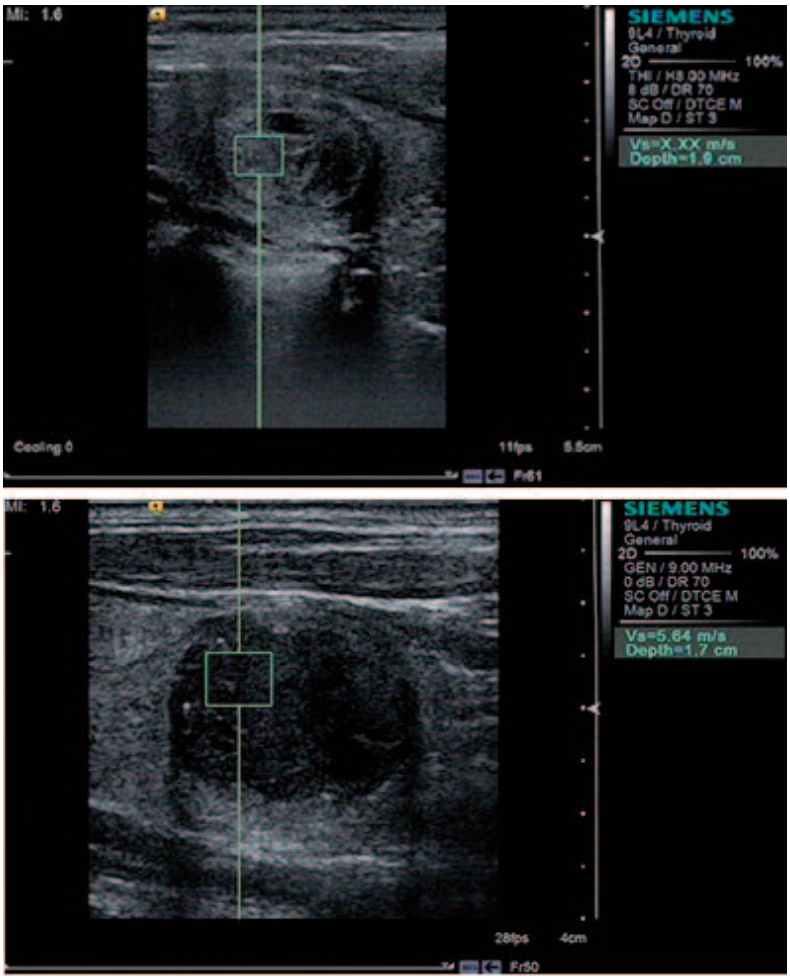

Figure 3. A, VTQ of the malignant nodule shows that SWV was x.xx ms-1; **B,** SWV of the benign nodules was 5.64 ms-1.

tween benign and malignant nodules. The shunt sensitivity and specificity (HFUS and ARFI) was 99.5% and 30%, respectively. All combined (US+ARFI+CEUS), the shunt sensitivity and specificity values were 99.7% and 20.6%, respectively (Table IV). In this study, the combined CEUS and US was better than CEUS or US alone, and the combined US, ARFI and CEUS was better than ARFI+CEUS. However, the US+ARFI+CEUS vs. US+ARFI and US+ARFI+CEUS vs. US+CEUS differed non-significantly.

Binary Logistic Regression Analysis

The pathological findings and the sonographic features were treated as independent variables. A binary logistic regression analysis was performed using forward stepwise method. The results of logistic regression analysis are summarized in Table V. The Wald χ^2-test for each regression coefficient showed that the *p*-values for morphology, mean SWV using ARFI, and T-max for perfusion of contrast agent were all <0.05 and could thus be used as independent variables in a logistic regression model using the following expression:

$$\text{Logit (P)} = -6.855+2.263X_3+1.001X_7+2.331X_8$$

The likelihood test for the above model (χ^2=33.366; $p < 0.05$) indicated that the model was statistically significant. The morphology, SWV, and T-max for perfusion of contrast agent were all identified as risk factors. This regression model could be used to determine whether the nodule was benign or malignant. If the regression *P*-value was >0.05, the nodule was predicted to be malignant; if not, the nodule was predicted to be benign. The predictive accuracy was 85.1% (68/80). The predicted area under the receiver operating characteristic (ROC) curve (Figure 5) was 0.945±0.033 (95%CI: 0.880-1.011; $p < 0.005$) for the same model used to determine the probability of malignancy.

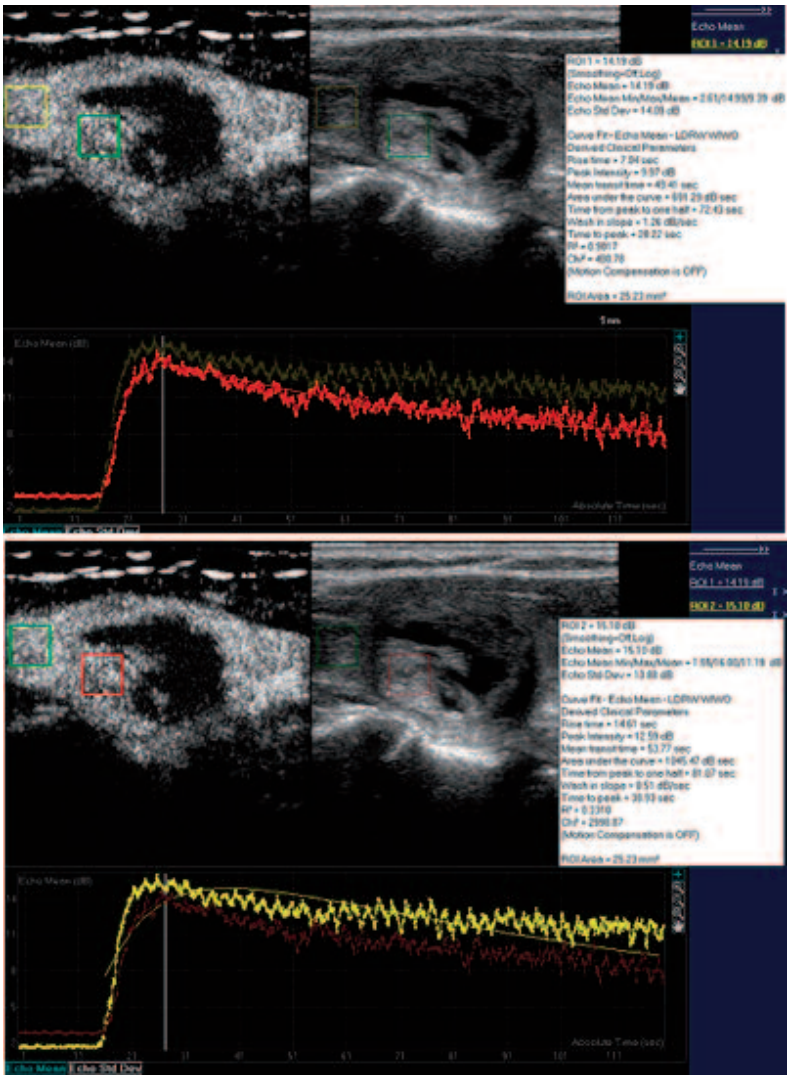

Figure 4. ***A,*** CEUS images of malignant nodules. Time-intensity curve (TIC) analysis of the malignant nodule: ROI for red line was placed in the malignant nodule; ***B,*** CEUS image of the adjacent thyroid tissue. TIC analysis: ROI for yellow line was placed in the adjacent thyroid tissue.

Discussion

Binary logistic regression analysis is widely used in different fields of medical research, including epidemiology, discriminant analysis of clinical diagnostic criteria and treatment evaluation[9]. Logistic regression is based on the assumption that a logistic relationship exists between the probability of group membership and one or more predictor variables[10]. It can be used to generate probabilities of class membership for each object. The present study utilized the binary logistic regression analysis to determine the relationships among HFUS, ARFI and CEUS imaging techniques herein used for diagnosis of thyroid nodules. The results of this study provide insight into the diagnostic criteria for thyroid nodules. OR can be used as a weighting measure for signs or as the basis for distinguishing between major and minor symptoms. Signs with an OR ≥3 (strong correlation) were classified as major, while those with an OR ≥1 but <3 were classified as minor. Symptoms/signs with an OR <1 (weak correlation) were ignored[11]. For instance, in terms of the diagnostic criteria for malignant thyroid nodules, the main symptom was TTP perfusion of CEUS (OR = 10.281), while mean SWV (OR = 2.721) for minor symptoms and morphology (OR = 0.104) were ignored. It was, therefore, concluded that the TTP and VTI were risk factors. Malignant nodules may have aspect ratio <1 or >1 or irregular. Regression analysis also helps filtering out the factors with real statistical significance from the multiple complex factors.

In modern imaging technology, HFUS plays an important role in the diagnosis of thyroid nod-

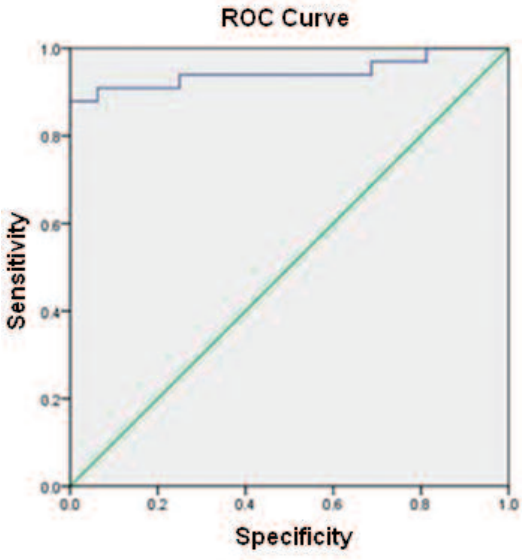

Figure 5. Receiver operating characteristic (ROC) curve of the malignant thyroid nodules is shown using Logistic regression model to determine the probability.

ules. Grayscale ultrasonography was reported to have clinical value to diagnose as well as distinguish between benign and malignant thyroid nodules[12]. The results of the present study are generally consistent with those of previous studies using dimensional B-mode ultrasonography. However, the sensitivity and specificity of HFUS differ dramatically, and there is no way to obtain information on the hardness of the diseased tissue. ARFI is an emerging technology that uses a region of interest (ROI) cursor to determine elasticity in the ROI during real-time imaging. Tissues incur lateral displacement to propagate shear wave by ARFI and SWV can be detected. The difference between ARFI and conventional strain elastography is that the ARFI can overcome certain shortcomings, such as the fact that surface compression elastography cannot exert any pressure on deeper tissues from the surface, and also that compression elastography can be affected by personal factors[13-15].

Measurement of the SWV value with VTQ gives a direct representation of this finding as the SWV value of malignant nodules was found to be higher than that of benign nodules (p = 0.029). The hardness of malignant nodules may be associated with their pathology, e.g. a thyroid papillary carcinoma with interstitial and vascular calcification is more fibrous which increases the hardness of the tumor. Meanwhile, malignant nodules can infiltrate and integrate closely with the surrounding tissues, which also results in increased hardness. Malignant nodules are prone to necrosis whereas benign lesions, such as nodular thyroid tumors, contain tumor cells that can form acini of different sizes with varying amounts of gum inside their cavity which reduces their hardness. Benign nodules (especially nods) are also prone to cystic changes. On the other hand, papillary thyroid carcinomas can be accompanied by nodular goiters and the proliferative changes in the papillary carcinoma associated with nodular goiter will involve relatively few tumor cells, thus the hardness of the nodule would not alter much and it would remain elastic.

Since it was difficult to obtain the quantitative indicators in CDUS, we used CEUS to show that the nodular enhancement differed from the normal tissue. The CEUS time-intensity curve can provide an indirect description of the blood supply inside nodules. CEUS may reflect biological characteristics, such as tumor growth and metastasis, and the perfusion of the contrast agent is dependent on the formation of new blood vessels[16]. The structure of blood vessels inside malignant nodules differs from the microvascular structure of normal tissue[17]. The neovascular structure inside malignant nodules is disordered and irregular whereas the vascular structure of benign nodules is similar to the normal tissue vasculature[18]. In addition, since disordered vessels cannot supply internal tissues uniformly, malignant nodules may suffer from liquefaction and necrosis. CEUS thus differs between benign and malignant nodules, based on the vascular structure and microcirculation[19].

CEUS indicated that the size of the nodules appeared to be closer to the size of the pathologic nodules. Other studies also showed that malignant nodules could rapidly reach the peak perfusion[20], but none has reported a statistically significant difference in the peak intensity and elimination values compared with benign nodules. In contrast, a previous study showed that the time-intensity curve did not enable differentiation of benign and malignant nodules[21].

These signs often have some degree of correlation (consistent with pathological finding). In this study, the internal organization form of nodules will affect the internal echogenicity; also it will affect the elasticity and CEUS. Notably, choice of the appropriate method is important for the evaluation of the combined test sensitivity. Two indexes in parallel can greatly improve the sensitivity, and by using more than three items in parallel, the sensitivity increased smoothly, according to the joint test (parallel) sensitivity estima-

tion formula. Therefore, in the actual combined examination, two or three parallel indexes are quite suitable.

Parallel test, refers to the simultaneous application of two trials in which the whole test becomes positive when either one of the tests is positive. The combination can improve the sensitivity, but reduce the specificity. On the other hand, in serial test, the whole test becomes positive only when all the tests are positive. The combination can improve the specificity, however, with the reduced sensitivity[22]. Therefore, we need to choose the test variables according to different situations. The sensitivity and specificity estimations of combined screening have theoretical and practical significance in epidemiology and clinical medicine. It thus remains difficult to compare findings from different studies. The ultimate goal is to distinguish the benign from the malignant nodules via a non-invasive technique and to reduce unnecessary thyroidectomies. As well, calcifications of nodules can affect the examination findings because the contrast agent cannot reach the calcified areas. There is no established standard for applying gentle force during elastography, and the imaging quality needs to be improved. VTI of ARFI image showed only the gray-scale image with no detailed data. Thus, we could not quantify to determine whether the nodule was hard or soft. Since the VTQ of ARFI was prone to be affected by breathing or carotid pulse, repeated measurements were required.

Conclusions

Binary logistic regression analysis can effectively screen the significant parameters for the differential diagnosis of benign and malignant thyroid nodules. Conjoint analysis of the specific features of thyroid nodules imaged by GSUS, ARFI, and CEUS enhanced the diagnostic value of thyroid nodules. Combining CEUS and US was better than using CEUS or US alone, and combining US, ARFI and CEUS was better than using ARFI plus CEUS. Using HFUS is also important, whereas using ARFI and CEUS improves the sensitivity of the diagnosis.

Acknowledgements

We thank all our colleagues from the Department of Ultrasound Medicine at Beijing Chaoyang Hospital, Capital Medical University, China for their kind support.

Conflict of Interest

The Authors declare that they have no conflict of interests.

References

1) Zhang YF, Xu HX, He Y, Liu C, Guo LH, Liu LN, Xu JM. Virtual touch tissue quantification of acoustic radiation force impulse: a new ultrasound elastic imaging in the diagnosis of thyroid nodules. PLoS One 2012; 7: e49094.
2) Ma JJ, Ding H, Xu BH, Xu C, Song LJ, Huang BJ, Wang WP. Diagnostic performances of various gray-scale, color Doppler, and contrast-enhanced ultrasonography findings in predicting malignant thyroid nodules. Thyroid 2014; 24: 355-363.
3) Ueno E, Ito A. Diagnosis of breast cancer by elasticity imaging. Eizo Joho Medical 2004; 36: 2-6.
4) Bojunga J, Dauth N, Berner C, Meyer G, Holzer K, Voelkl L, Herrmann E, Schroeter H, Zeuzem S, Friedrich-Rust M. Acoustic radiation force impulse imaging for differentiation of thyroid nodules. PLoS One 2012; 7: e42735
5) Sporea I, Sirli R, Bota S, Vlad M, Popescu A, Zosin I. ARFI elastography for the evaluation of diffuse thyroid gland pathology: Preliminary results. World J Radiol 2012; 4: 174-178.
6) Claudon M, Cosgrove D, Albrecht T, Bolondi L, Bosio M, Calliada F, Correas JM, Darge K, Dietrich C, D'Onofrio M, Evans DH, Filice C, Greiner L, Jäger K, Jong Nd, Leen E, Lencioni R, Lindsell D, Martegani A, Meairs S, Nolsøe C, Piscaglia F, Ricci P, Seidel G, Skjoldbye B, Solbiati L, Thorelius L, Tranquart F, Weskott HP, Whittingham T. Guidelines and good clinical practice recommendations for contrast enhanced ultrasound (CEUS). Ultraschall Med 2008; 29: 28-44.
7) Piscaglia F, Bolondi L. The safety of Sonovue in abdominal applications: retrospective analysis of 23188 investigations. Ultrasound Med Biol 2006; 32: 1369-1375.
8) Massimo G, Davide O, Giulia M, Barbara M, Enzo S, Francesco M, Gianni T. Is there a real diagnostic impact of elastosonography and contrast-enhanced ultrasonography in the management of thyroid nodules? J Zhejiang Univ-Sci B (Biomed & Biotechnol) 2013; 14: 195-206.
9) Asteria C, Giovanardi A, Pizzocaro A, Cozzaglio L, Morabito A, Somalvico F, Zoppo A. US-elastography in the differential diagnosis of benign and malignant thyroid nodules. Thyroid 2008; 18: 523-531.
10) Hosmer D.W, Lemeshow S. Applied Logistic Regression, Wiley, New York, 1989.
11) Yao KW, He QY, Teng F, Wang J. Logistic regression analysis of syndrome essential factors in patients with unstable angina pectoris. J Tradit Chinese Med 2011; 31: 273-276.
12) Gharib H, Papini E, Paschke R, Duick DS, Valcavi R, Hegedüs L, Vitti P; AACE/AME/ETA Task Force on Thyroid Nodules. American Association of Clinical Endocrinologists, Associazione Medici En-

docrinologi, and European Thyroid Association medical guidelines for clinical practice for the diagnosis and management of thyroid nodules. Endocr Pract 2010; 16: 468-475.

13) Mauldin FW, Zhu HT, Behler RH, Nichols TC, Gallippi CM. Robust principal component analysis and clustering methods for automated classification of tissue response to ARFI excitation. Ultrasound Med Biol 2008; 34: 309-325.

14) Nightingale K, Soo MS, Nightingale R, Trahey G. Acoustic radiation force impulse imaging: in vivo demonstration of clinical feasibility. Ultrasound Med Biol 2002; 28: 227-235.

15) Wells PNTW and Liang HD. Medical ultrasound: imaging of soft tissue strain and elasticity. J R Soc Interface 2011; 8: 1521-1549.

16) Chaudhari MH, Forsberg F, Voodarla A, Saikali FN, Goonewardene S, Needleman L, Finkel GC, Goldberg BB. Breast tumor vascularity identified by contrast enhanced ultrasound and pathology: initial results. Ultrasonics 2000; 38: 105-109.

17) McDonald DM and Foss AJ. Endothelial cells of tumor vessels: abnormal but not absent. Cancer Metastasis Rev 2000; 19: 109-120.

18) Görges R, Eising EG, Fotescu D, Renzing-Köhler K, Frilling A, Schmid KW, Bockisch A, Dirsch O. Diagnostic value of high-resolution B-mode and power-mode sonography in the follow-up of thyroid cancer. Eur J Ultrasound 2003; 16: 191-206.

19) Argalia G, de Bernardis S, Mariani D, Abbattista T, Taccaliti A, Ricciardelli L, Faragona S, Gusella PM, Giuseppetti GM. Ultrasonographic contrast agent: evaluation of time intensity curves in the characterisation of solitary thyroid nodules. Radiol Med 2002; 103: 407-413.

20) Zhang B, Jiang YX, Liu JB, Yang M, Dai Q, Zhu QL, Gao P. Utility of contrast-enhanced ultrasound for evaluation of thyroid nodules. Thyroid 2010; 20: 51-57.

21) Friedrich-Rust M, Sperber A, Holzer K, Diener J, Grünwald F, Badenhoop K, Weber S, Kriener S, Hermann E, Bechstein WO, Zeuzem S, Bojunga J. Real-time elastography and contrast-enhanced ultrasound for the assessment of thyroid nodules. Exp Clin Endocrinol Diabetes 2010; 118: 602-609.

22) Bernard AR. Fundamentals of Biostatistics. Cengage Learning, 2006.